Novel *FRMD7* Mutations and Genomic Rearrangement Expand the Molecular Pathogenesis of X-Linked Idiopathic Infantile Nystagmus

Basamat AlMoallem,[1,2] Miriam Bauwens,[1] Sophie Walraedt,[3] Patricia Delbeke,[3] Julie De Zaeytijd,[3] Philippe Kestelyn,[3] Françoise Meire,[4] Sandra Janssens,[1] Caroline van Cauwenbergh,[1] Hannah Verdin,[1] Sally Hooghe,[1] Prasoon Kumar Thakur,[1] Frauke Coppieters,[1] Kim De Leeneer,[1] Koenraad Devriendt,[5] Bart P. Leroy,[1,3,6] and Elfride De Baere[1]

[1]Center for Medical Genetics, Ghent University Hospital, Ghent, Belgium
[2]Department of Ophthalmology, King Abdul-Aziz University Hospital, College of Medicine, King Saud University, Riyadh, Saudi Arabia
[3]Department of Ophthalmology, Ghent University Hospital, Ghent, Belgium
[4]Department of Ophthalmology, Queen Fabiola Children's University Hospital, Brussels, Belgium
[5]Center for Human Genetics, Leuven University Hospitals, Leuven, Belgium
[6]Division of Ophthalmology, The Children's Hospital of Philadelphia, Philadelphia, Pennsylvania, United States

Correspondence: Elfride De Baere, Center for Medical Genetics, Ghent University Hospital, De Pintelaan 185, B-9000 Ghent, Belgium; elfride.debaere@ugent.be.

Submitted: October 26, 2014
Accepted: February 5, 2015

Citation: AlMoallem B, Bauwens M, Walraedt S, et al. Novel *FRMD7* mutations and genomic rearrangement expand the molecular pathogenesis of X-linked idiopathic infantile nystagmus. *Invest Ophthalmol Vis Sci*. 2015;56:XXX–XXX. DOI:10.1167/iovs.14-15938

Purpose. Idiopathic infantile nystagmus (IIN; OMIM 31700) with X-linked inheritance is one of the most common forms of infantile nystagmus. Up to date, three X-linked loci have been identified, Xp11.4-p11.3 (calcium/calmodulin-dependent serine protein kinase [*CASK*]), Xp22 (*GPR143*), and Xq26-q27 (*FRMD7*), respectively. Here, we investigated the role of mutations and copy number variations (CNV) of *FRMD7* and *GPR143* in the molecular pathogenesis of IIN in 49 unrelated Belgian probands.

Methods. We set up a comprehensive molecular genetic workflow based on Sanger sequencing, targeted next generation sequencing (NGS) and CNV analysis using multiplex ligation–dependent probe amplification (MLPA) for *FRMD7* (NM_194277.2) and *GPR143* (NM_000273.2).

Results. In 11/49 probands, nine unique *FRMD7* changes were found, five of which are novel: frameshift mutation c.2036del, missense mutations c.801C>A and c.875T>C, splice-site mutation c.497+5G>A, and one genomic rearrangement (1.29 Mb deletion) in a syndromic case. Additionally, four known mutations were found: c.70G>A, c.886G>C, c.910C>T, and c.660del. The latter was found in three independent families. In silico predictions and segregation testing of the novel mutations support their pathogenic effect. No *GPR143* mutations or CNVs were found in the remainder of the probands (38/49).

Conclusions. Overall, genetic defects of *FRMD7* were found in 11/49 (22.4%) probands, including the first reported genomic rearrangement of *FRMD7* in IIN, expanding its mutational spectrum. Finally, we generate a discovery cohort of IIN patients potentially harboring either hidden a variation of *FRMD7* or mutations in genes at known or novel loci sustaining the genetic heterogeneity of IIN.

Keywords: *FRMD7* mutations, idiopathic infantile nystagmus, next generation sequencing, MLPA, genomic rearrangement

Idiopathic Infantile nystagmus (IIN; MIM# 310700) is one of the most common forms of infantile nystagmus with an estimated prevalence of 1.9 per 10,000 in Leicestershire and Rutland, United Kingdom.[1] IIN is characterized by bilateral uncontrollable ocular oscillation occurring mostly in horizontal plane of either jerk or pendular waveform. It arises independently of any ocular or neurological abnormalities and often leading to low visual acuity scores due to excessive movement of the image away from the fovea. Patients with IIN may develop abnormal head posture (torticollis) when the null zone is not at the primary gaze position.[2]

The inheritance patterns of IIN are heterogeneous with X-linked inheritance as the most frequent one (OMIM 31700). Up to date three X-linked loci have been identified, more specifically at Xp11.4-p11.3, Xp22, and Xq26-q27, respectively. Recently Hackett et al.[3] reported mutations in the calcium/calmodulin-dependent serine protein kinase (*CASK*) gene, located at Xp11.4–p11.3, in patients with X-linked IIN and mental retardation.[3] The *GPR143* gene, located at Xp22, is known to be mutated in ocular albinism (OA), invariably characterized by infantile nystagmus. *GPR143* mutations have also been found however to cause a variant form of OA with IIN as the most prominent and only consistent finding without the classical OA manifestations.[4,5]

In approximately 20% to 97% of X-linked IIN cases, mutations can be found in the FERM domain-containing 7 gene (*FRMD7*) located at Xq26-q27 (NYS1 locus).[6–10] Due to skewed

X-chromosome inactivation, approximately one-half of the heterozygote females are mildly affected.[11]

The *FRMD7* gene comprises 12 exons and encodes a protein of 714 amino acids, which is a member of the FERM domain family of plasma membrane cytoskeleton coupling proteins. As in most other members, the conserved FERM domain of FRMD7 is located at the N-terminus and is divided into three lobes (F1–F3) that form a cloverleaf structure. This domain is usually responsible for membrane association through interaction with integral membrane proteins and lipids. In contrast to the N-terminus, the C-terminal domain of FRMD7 bears no significant homology to other proteins. FRMD7 also has a central FERM-adjacent (FA) domain that is found in a subset of FERM domain proteins, and which has been found to regulate protein function through modifications such as phosphorylation.[12,13]

FRMD7 is expressed in both the developing neural retina and in developing ocular motor structures such as the cerebellum and vestibulo-optokinetic system and it has been found to play a role in control of eye movement and gaze stability.[7]

In differentiating mouse neuroblastoma Neuro-2a cells, FRMD7 colocalizes with the actin of primary neurites. FRMD7 overexpression in these cells promotes neurite outgrowth,[14] while knockdown of *FRMD7* causes a reduction in average neurite length.[15] Watkins et al.[15] recently found an interaction between FRMD7 and CASK. One of the functions of CASK in neurons is to link the plasma membrane to the actin cytoskeleton. It is hypothesized that *FRMD7* mutations could act by disrupting the interaction between FRMD7 and CASK.[15]

Whether the primary disease underlying IIN is an afferent visual disorder disturbing foveal vision during development is still a matter of debate. Using high-resolution retinal imaging such as optical coherence tomography (OCT) it has been shown that retinal deficits exist in individuals with IIN.[8] Recently, an extensive study investigated the retinal morphology in patients with FIN and showed an association between *FRMD7* mutations and isolated foveal hypoplasia.[8]

This opens the possibility that the primary pathology behind most forms of IIN could be sensory in origin.

To determine the role of coding *FRMD7* and *GPR143* mutations and CNVs in a Belgian IIN cohort, we set up a comprehensive molecular genetic workflow based on Sanger sequencing and targeted next generation sequencing (NGS), copy number variation (CNV) screening including multiplex ligation–dependent probe amplification (MLPA) and microarray-based comparative genomic hybridization (arrayCGH). We performed extensive variant interpretation for the evaluation of missense variants and conducted haplotype analysis for a recurrent frameshift mutation.

Methods

Patients and Clinical Assessment

Forty-nine unrelated consenting Belgian families were recruited from the ophthalmology clinics at the Ghent University Hospital, Belgium (21 familial cases, 28 sporadic cases). Routine clinical examination and ophthalmic evaluation included in most cases best-corrected visual acuity (BCVA) measurements; slit-lamp biomicroscopy, color vision test, Goldmann visual fields, fundoscopy, OCT, and ERG.

Mutation Screening by Sanger Sequencing

Genomic DNA was extracted from peripheral venous blood using standard procedures. Primers for PCR amplification of the coding region and splice site junctions of *FRMD7* were designed and can be found in Supplementary Table S1. Sanger sequencing was performed according to the manufacturer's instructions (BigDye Terminator v3.1 Cycle Sequencing Kit; ABI 3730XL genetic Analyzer; Applied Biosystems, Carlsbad, CA, USA). The reference sequence used is NM_194277.2.

Variant Interpretation

In Silico Predictions. Alamut v2.4 gene browser with relevant annotations gathered from public databases (from the National Center for Biotechnology Information [NCBI], the University of California, Santa Cruz [UCSC] and the European Bioinformatics Institute [EBI]) was used. Functional impact of variants was assessed using the following prediction tools: splice prediction tools (SpliceSiteFinder-like, MaxEntScan, NNSPLICE), missense prediction tools (Align GVGD, Sorting Intolerant From Tolerant [SIFT], MutationTaster, and PolyPhen-2).

Molecular Structural Modeling of Missense Mutations. The primary sequence of human FRMD7 was obtained from the Swissprot database Uniprot ID: 3Q6ZUT. The template PDB ID: 2HE7 for FERM domain residues 2 to 282 was selected, having 41% identity using BlastP against the Protein Databank for FERM domains.[16] However, due to lack of significant sequence identity for the FA domain residues 288 to 336, we relied on fold recognition algorithm to identify remote homologous template. We have retrieved the template PDB ID: 1E5W, confidence 58% and coverage: 47% for the FA domain using Phyre2 fold recognition server.[17] The three-dimensional (3D) models were constructed for FRMD7 residues 1 to 336 by means of homology modeling using MODELLER 9.12 with selected templates.[18] The overall stereochemical quality of the model was assessed on the SAVS server (in the public domain, http://nihserver.mbi.ucla.edu/SAVES/). Interaction analysis was performed by the contact program of the CCP4 package. The molecular visualization of the FRMD7 model was done using PyMol.

Haplotype Analysis

Haplotype reconstruction was performed by genotyping microsatellite markers flanking the *FRMD7* gene. The microsatellite markers were selected from the combined Genethon, Marshfield, and deCODE genome browser (NCBI, Bethesda, MD, USA) and PCR amplified. The sequence-specific forward primer is provided with an M13-tail (5′-cacgacgttgtaaaacgac-3′) on which a universal M13-primer can bind while the sequence-specific reverse primer is not bound. Data were analyzed using the GeneMapper software (Applied Biosystems). Pedigree and haplotype construction were done using Progeny software (Progeny Software LLC, Delray Beach, FL, USA).

Mutation Screening by Next Generation Sequencing (NGS)

Targeted NGS was optimized for *FRMD7* and *GPR143* using a workflow described by De Leene-er et al.[19] Previously developed *FRMD7* PCR primers and Sanger-identified variants were used in seven patients for validation. The PCR products were pooled per patient and quantified using the LabChip GX (Caliper Life Sciences, Hopkinton, MA, USA) and pooled equimolarly with other PCR products into combination pools. The combination pools were purified (Agencourt AMPure XP beads Beckman Coulter, Brea, CA, USA) and their concentration was measured (Qubit with the Quant-iT ds DNA HS assay kit; Life Technologies, Carlsbad, CA, USA). Next, sample preparation and indexing was performed using the NexteraXT DNA sample preparation and Index kits (Illumina, San Diego,

Investigative Ophthalmology & Visual Science

CA, USA) according to the manufacturer's instructions, followed by a quality control on the Bioanalyzer 2100 (Agilent technologies, Santa Clara, CA, USA). Then, the indexed pools were normalized using the Kapa Library Quantification Kit (KAPA Biosystems, Woburn, MA, USA), and pooled into one final pool. This pool was subsequently sequenced on a MiSeq (Illumina) at 2 × 250 bp read length configuration and dual indexing. Finally, CLC Genomics Workbench (CLCBio, Aarhus, Denmark) was used for the mapping of the reads and data analysis of the variants.

Multiplex Ligation–Dependent Probe Amplification (MLPA)

FRMD7. Multiplex ligation–dependent probe amplification was performed using the SALSA P269 *FRMD7*-NYS1 probe kit containing 28 MLPA probes with amplification products between 166 and 391 nucleotides, following the manufacturer's protocol (MRC-Holland, Amsterdam, Holland).

GPR143. Multiplex ligation–dependent probe amplification was performed using the SALSA P054 *FOXL2-TWIST1*-Lot 0905 kit containing 34 MLPA probes with amplification products between 139 and 436 nucleotides, following the manufacturer's protocol (MRC-Holland).

Microarray-Based Comparative Genomic Hybridization (arrayCGH)

Genome-wide copy number profiling was performed on 180K oligonucleotide arrays (Agilent Technologies). Hybridizations were performed according to manufacturer's instructions with minor modifications. The results were subsequently visualized in arrayCGHbase.[20]

Results

Clinical Assessment

Forty-nine unrelated Belgian probands with IIN were investigated in our study. In these families, the disease was transmitted either from a female carrier to an affected son ($n = 21$) or occurred isolated ($n = 28$). There was no male-to-male transmission, excluding autosomal dominant inheritance. All participants underwent detailed ophthalmic evaluation. The clinical characteristics of the affected individuals in which *FRMD7* mutation was found, are summarized in Table 1.

FRMD7 Mutation Screening

Sanger Sequencing. Sanger sequencing of *FRMD7* in this Belgian cohort revealed eight unique mutations in 10 unrelated families. Four of these are novel: frameshift mutation c.2036del p.(Leu679Argfs*8), missense mutations c.801C>A p.(Phe267-Leu) and c.875T>C p.(Leu292Pro) and splice-site mutation c.497+5G>A. Additionally, four known mutations were found: missense mutations c.70G>A p.(Gly24Arg) and c.886G>C p.(Gly296Arg), nonsense mutation c.910C>T p.(Arg304*); frameshift mutation and c.660del p.(Asn221Ilefs*11), which were found in three independent families. Figure 1 represents the pedigrees and the molecular genetic data. A schematic diagram of the *FRMD7* gene structure and the protein domains with these identified mutations are represented in Figure 2A.

Variant Interpretation

In Silico Predictions. Predictions using SIFT, MutationTaster, PolyPhen-2, and splicing tools suggest that the identified variants in *FRMD7* have a pathogenic effect on protein function. Moreover, we showed absence of these missense variants in different genomic databases (dbSNP, 1000 genomes, and IVS) except for c.70G>A p.(Gly24Arg), known as rs137852210 in dbSNP and assigned as pathogenic allele. An overview of these variants and their predictions is given in Table 2.

Structural Molecular Modeling of Missense Mutations. The mutated residues of the four missense mutations identified, p.(Gly24Arg), p.(Phe267Leu), p.(Leu292Pro), and p.(Gly296Arg), are all highly conserved (Fig. 2B). Structural modeling of these missense mutations is summarized in Figure 2C and suggests a pathogenic effect of all the missense mutations identified.

Haplotype Analysis of c.660del Mutants

This recurrent deletion was found in affected males of three unrelated families F4, 5, and 6, respectively. To assess whether the occurrence of this mutation in these three families arose independently or by a common founder, we performed haplotype reconstruction using microsatellite markers flanking *FRMD7*. Based on the different haplotypes in the affected individuals, there are no strong arguments for a founder effect so far (Fig. 1B).

Targeted NGS

To develop an NGS-based test for molecular genetic assessment of the coding region of *FRMD7,* we implemented the primers developed for Sanger sequencing in a flexible workflow of targeted NGS developed in our lab.[19] For the initiation of this step we sequenced material for seven unique *FRMD7* mutations previously found by Sanger sequencing. The minimum coverage of all *FRMD7* targets is 38×.[19] All seven mutations were validated using this targeted NGS strategy, an illustration of which can be found in Figure 3.

Copy Number Screening

MLPA. To exclude *FRMD7* copy number variations in the remaining probands without coding *FRMD7* mutations, 38/49 (77.6%) probands, including 16 females and 22 males, underwent MLPA using a probe for each coding exon and for the upstream and downstream region of *FRMD7*. No CNVs of *FRMD7* were found using this approach.

ArrayCGH. In one case, more specifically in a 14-year-old male, arrayCGH was performed because of a diagnosis of autism spectrum disorder and global developmental delay. In addition, he displayed nystagmus from the age of 1.5 years. A 370-kb duplication of chromosome band 7q22.1 and a 1.29 Mb deletion of chromosome band Xq26.1q26.2 were found: arr 7q22.1q22.1(98274806-98598214)x3, and arr Xq26.1q26.2(129928356-131292675)x0. The deleted region contains *FRMD7* and six other genes: *ENOX2, ARHGA36, IGSF1, OR13H1, FIRRE*, and *MST4*. Apart from *FRMD7*, only the *IGSF1* gene is associated with a disease, more specifically with central hypothyroidism and testicular enlargement syndrome (OMIM 300888). Segregation analysis showed this deletion was inherited from the mildly affected mother. In addition, a maternal aunt and her daughter were mildly affected. No thyroid or puberty problems have been reported in the family. Noteworthy, the proband displayed retarded meconium evacuation after birth, which required a stoma.

To evaluate the prevalence of CNVs of the *FRMD7* region and associated phenotypes, we investigated the Database of

Investigative Ophthalmology & Visual Science

Table 1. Overview of the *FRMD7* Mutations and Their Associated Phenotypes

Family	ID	Sex	Age	Mutation	BCVA		Slit-Lamp Biomicroscopy	Fundus Copy	Color Vision	Goldmann Visual Fields	Nystagmus	Torticollis	OCT	ERG
					OD	OS								
F1	II:1*	Male	15 y	c.70G>A	8/10	8/10	Normal/no iris transillumination	Normal	Normal	Normal	Pendular	Yes	Normal foveal pit	Normal
	I:2	Female	34 y		–	–	–	–	–	–	–	–	–	–
F2	II:1*	Female	12 y	c.910C>T	7/10	7/10	Normal/no iris transillumination	Normal	Normal	Normal	Jerk	Yes	Normal foveal pit	Normal
F3	II:1*	Male	1 y	c.886G>C	6/10	8/10	Mild iris transillumination	Normal	Normal	Normal	Jerk	Yes	Normal foveal pit	Normal
F4	III:1	Female	41 y	c.660del	–	–	–	–	–	–	–	–	–	–
	IV:1*	Male	13 y		5/10	7/10	Normal/no iris transillumination	Normal	Normal	Normal	Pendular	Yes	–	–
	IV:2	Male	11 y		3/10	3/10	Normal/no iris transillumination	Normal	Normal	Normal	Pendular	Yes	–	–
F5	V:7*	Male	10 y		2/10	2/10	Normal/no iris transillumination	Normal	Normal	Normal	Jerk	Yes	–	–
	IV:6	Female	37 y		5/10	7/10	Normal/no iris transillumination	Normal	Normal	Normal	No nystagmus	No	–	–
F6	IV:2	Female	34 y		–	–	–	–	–	–	–	–	–	–
	V:1*	Male	9 y		2/10	2/10	Discrete peripheral iris transillumination	Normal	–	–	Jerk	No	Normal foveal pit	–
F7	III:1*	Male	2 y	c.2036del	6/10	6/10	Moderate lens opacification	Normal	Normal	Normal	Jerk	Yes	Normal foveal pit	–
	II:1	Female	30 y		–	–	–	–	–	–	–	–	–	–
	I:1	Male	80 y		–	–	–	–	–	–	–	–	–	–
F8	II:1*	Female	43 y	c.801C>A	4/10	6/10	Normal/no iris transillumination	Normal	Normal	Normal	–	–	–	–
F9	II:1*	Male	4 y	c.875T>C	9/10	9/10	Normal/no iris transillumination	Normal	–	–	Pendular	–	–	–
	I:2	Female	46 y		–	–	–	–	–	–	No nystagmus	No		
F10	IV:1*	Male	10 y	c.497+5G>A	2.5/10	2.5/10	Normal/no iris transillumination	Normal	Normal	Normal	Pendular	–	–	–

Overview of the clinical data found in 10 unrelated Belgian families with *FRMD7* mutations.

* Proband.

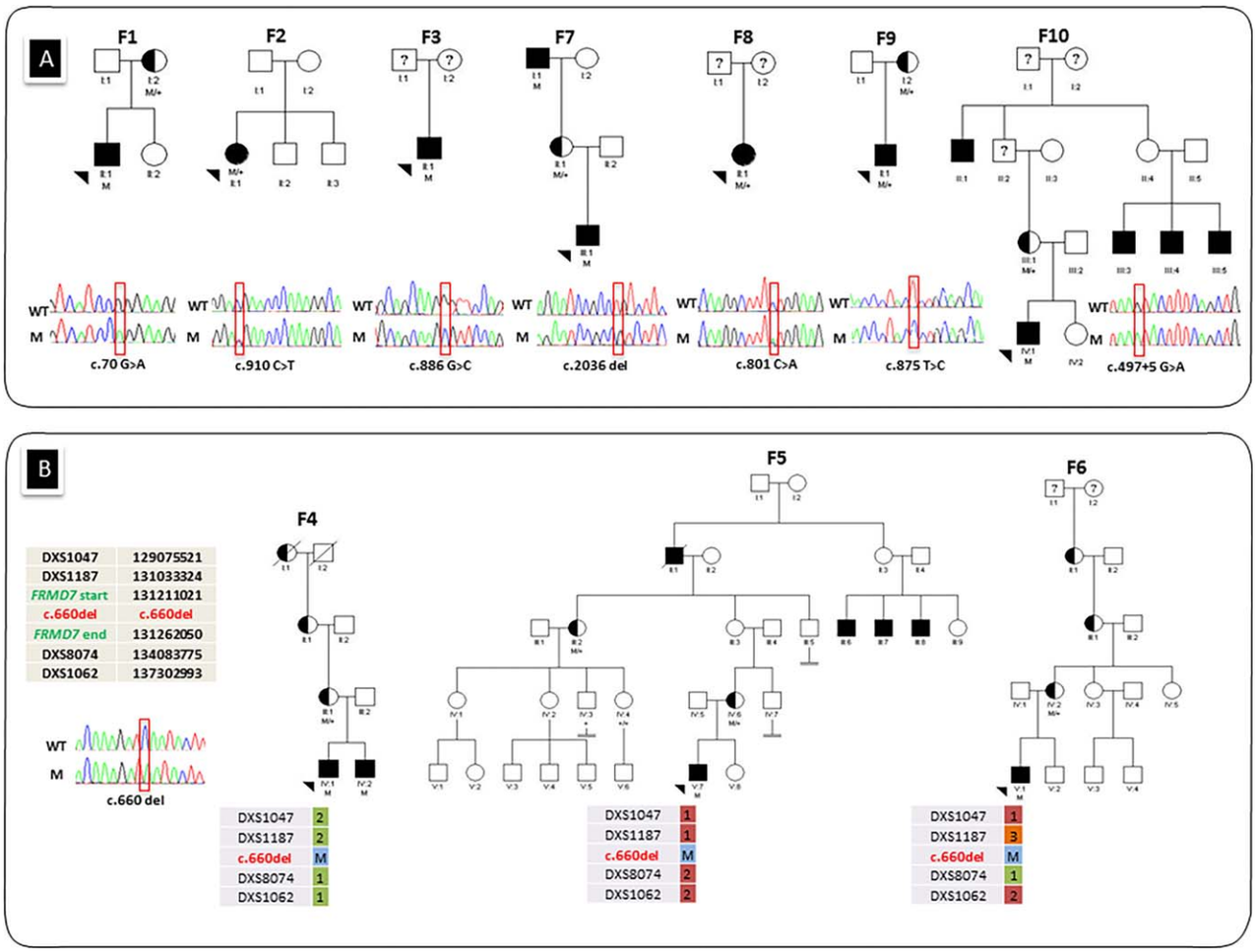

Figure 1. (**A**) Pedigrees of affected families (F1, F2, F3, F7, F8, F9, and F10) with IIN. *Filled symbols* indicate affected individuals, *half shaded symbols* indicate heterozygous carriers, *empty symbols* indicate unaffected individuals while an "*?*" *symbol* indicates an unknown status. The probands are highlighted by an *arrow*. Sequence electropherograms are represented underneath each pedigree. (**B**) Pedigrees of families (F4, F5, F6, and F7) with recurrent mutation c.660del. The pedigree and sequence electropherograms are represented as described in (**A**). The markers order and distances between the markers were retrieved from NCBI. WT, wild type; M, mutant.

Chromosomal Imbalance and Phenotype in Humans Using Ensemble Resources (Decipher), and our local arrayCGH database respectively. Twenty-two losses and 18 gains were found respectively, but IIN was not listed among the phenotypes (Fig. 4; Supplementary Table S2).

Apart from the 1.29-Mb deletion, no other CNVs of the *FRMD7* region were found in our local arrayCGH database.

GPR143 Mutation Screening

Targeted NGS. To exclude the possibility of missed X-linked ocular albinism in the remaining 38/49 (77.6%) probands without any coding *FRMD7* mutation or deletion, we screened the coding region of *GPR143* based on targeted NGS.[19] The minimum coverage of all *GPR143* targets is 38×.[19] No coding *GPR143* mutations were found using this approach.

Copy Number Screening by MLPA

To rule out *GPR143* CNVs in the 38/49 (77.6%) probands without coding *GPR143* mutations including 16 females and 22 males, we performed MLPA using a probe for each coding exon and for the upstream and downstream region of *GPR143*. No CNVs of *GPR143* were found using this approach.

Discussion

Coding *FRMD7* mutations and a genomic rearrangement were found in 11/49 (22.4%) of our total IIN cohort, supporting that *FRMD7* is a common cause of IIN and is in agreement with previous mutation studies.[21–23] We observed a difference in mutation detection rate between familial (7/21, 33.3%) and sporadic (4/28, 14.3%) cases. This difference was also noticeable in the original cloning paper of *FRMD7* by Tarpey et al.[7] in which the detection rate of the familial cases (24/26, 84.6%) was higher than the sporadic ones (3/42, 7%). In addition, we minimized the possibility of X-linked ocular albinism in the remaining overall cohort (38/49, 77.6%) as no coding *GPR143* mutations or deletions were found.

Of the four missense mutations found here, two are novel, p.(Phe267Leu) and p.(Leu292Pro). Apart from their location in highly conserved regions, the molecular structural modeling of all missense mutations suggests they may lead to deregulation of FRMD7: (1) p.(Gly24Arg) is located in the core region of the F1-FERM domain, likely destabilizing the protein by the

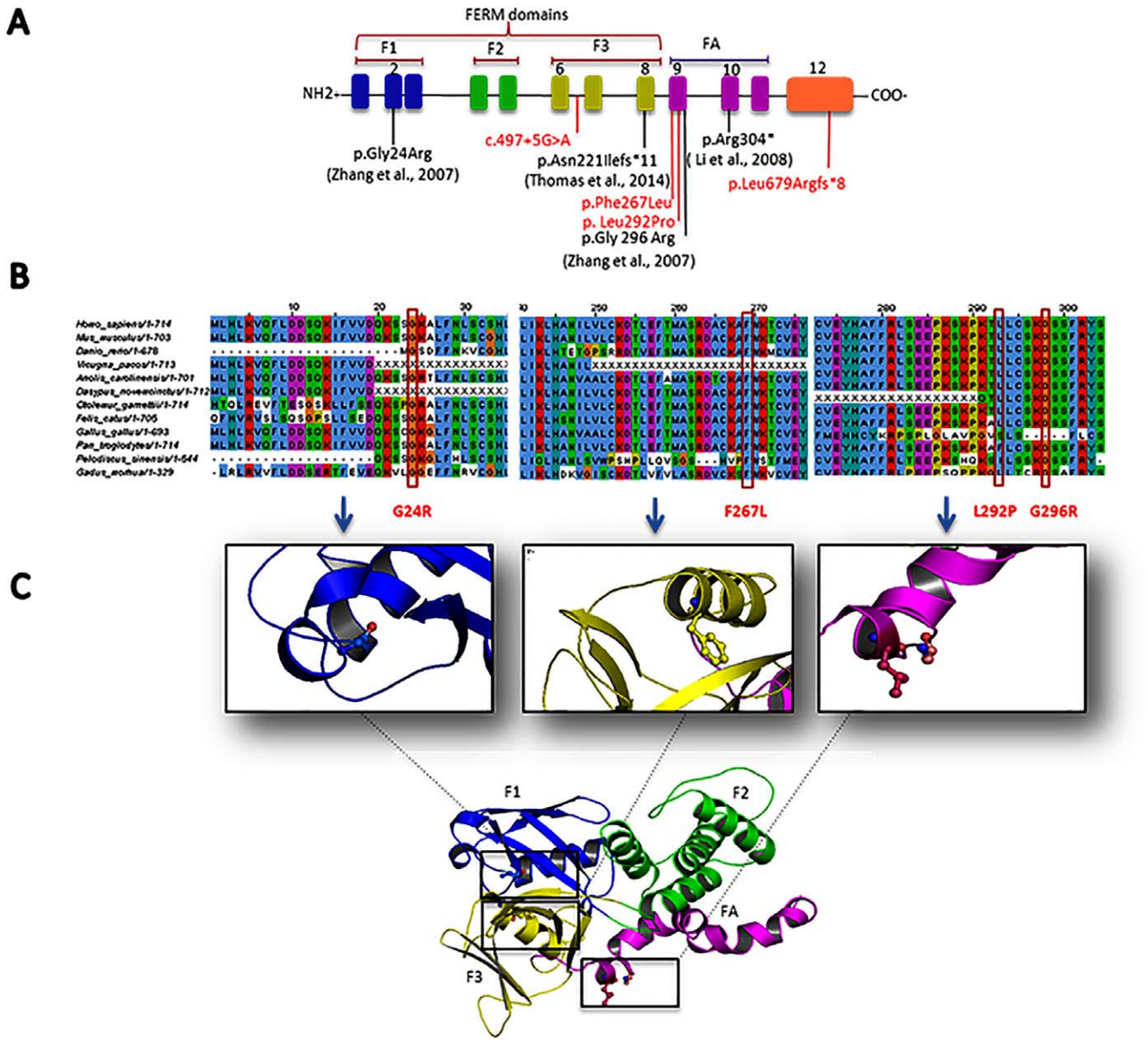

Figure 2. (**A**) Schematic representation of the *FRMD7* gene structure and the protein domains. It contains FERM domains (F1, F2, and F3) and FA. The numbers indicate the exon positions. The *arrows* indicated at the bottom of the figure represent *FRMD7* mutations. *Black arrows* indicate known mutations and *red arrows* indicate novel mutations. (**B**) Multiple sequence alignment of the FRMD7 protein in different species. The alignment of amino acids around residue p.24, p.267, p.292, and p.296 reveal evolutionary conservation of these residues. The *red boxes* in the alignment highlight amino acid residues affected by missense mutations. (**C**) Structure protein modeling of FRMD7. The positions of the missense mutations around residues p.24, p.267, p.292, and p.296 of FRMD7 are highlighted.

introduction of a larger amino acid within a restricted area of the protein,[24,25] (2) p.(Phe267Leu) is located in the middle of the F3 subdomain and may disrupt the aromatic interactions with the surrounding aromatic, positively charged and sulphur containing residues, thus potentially disrupting its binding site with other interacting partners and lipids.[26,27] The importance of aromatic–aromatic, aromatic–sulphur, and cation–π interactions in the structure and function of proteins is well established.[8–11] Exploring interactions in the middle of the Phe267 showed that aromatic amino acids (Phe238 and Trp268), sulphur-containing amino acids (Cys264 and Cys271), and positively-charged amino acids (His192, Lys265, and Lys269) are present within 3.5 Å of the Phe267. The p.(Phe267Leu) mutation is expected to lead to changes in aromatic interactions, that may perturb the protein and potentially disrupt its binding sites for interacting partners and lipids, and (3) both p.(Leu292Pro) and p.(Gly296Arg) are located in the FA domain. The p.(Leu292Pro) substitution may lead to change in α-helix conformation of the FA domain due to lack of a hydrogen on the amino group of Pro and can also affect the recognition specificity of the hydrophobic ligands[28,29] while p.(Gly296Arg) is likely to destabilize the protein by addition of a larger charged residue into the core of the FA domain of FRMD7. Moreover, the FA domain has also been found to regulate protein function through modifications such as phosphorylation and ubiquitination. Interestingly, Lys295 is involved in the ubiquitination[12] and the bulky side chain of Arg in p.(Gly296Arg) may obstruct the ubiquitination of Lys295.

Investigative Ophthalmology & Visual Science

Table 2. Overview of the *FRMD7* Mutations Found and Their Evaluation

Family	ID	Sex	Mutation	Protein Change	State	Exon/ Intron	In Silico Predictions				dbSNP/ EVS/1000 Genomes	Splicing Effect	Domain Affected	References
							Grantham	SIFT	PolyPhen	Mutation Taster				
F1	II:1*	M	c.70G>A	p.(Gly24Arg)	Hemizygous	Exon 2	125	Deleterious (score: 0.00)	Probably damaging	Disease causing (*P* value: 1.0)	rs137852210 (described as Pathogenic allele)	–	FERM 1	(Zhang et al., 2007) This study
	I:2	F			Heterozygous									
F2	II:1*	F	c.910C>T	p.(Arg304*)	Heterozygous	Exon 10	–	–	–	–	–	–	FA	(Li et al., 2008) This study
F3	II:1*	M	c.886G>C	p.(Gly296Arg)	Hemizygous	Exon 9	125	Deleterious (score: 0.00)	Probably damaging	Disease causing (*P* value: 1.0)	–	–	FA	(Zhang et al., 2007) This study
F4	III:1	F	c.660del	p.(Asn221Ilefs*11)	Heterozygous	Exon 8	–	–	–	–	–	–	FERM 3	(Thomas et al., 2014) This study
	IV:1*	M			Hemizygous									
	IV:2	M			Hemizygous									
F5	V:7*	M			Hemizygous									
	IV:6	F			Heterozygous									
	III:2	F			Heterozygous									
F6	IV:2	F			Heterozygous									
	V:1*	M			Hemizygous									
F7	III:1	M	**c.2036del**	**p.(Leu679Argfs*8)**	Hemizygous	Exon 12	–	–	–	–	–	–	C-terminal	**This study**
	II:1	F			Heterozygous									
	I:1	M			Hemizygous									
F8	II:1*	F	**c.801C>A**	**p.(Phe267Leu)**	Heterozygous	Exon 9	22	Deleterious (score: 0.00)	Probably damaging	Disease causing (*P* value: 1.0)	–	–	FA	**This study**
F9	II:1*	M	**c.875T>C**	**p.(Leu292Pro)**	Hemizygous	Exon 9	98	Deleterious (score: 0.00)	Probably damaging	Disease causing (*P* value: 1.0)	–	–	FA	**This study**
	I:2	F			Heterozygous									
F10	IV:1*	M	**c.497+5G>A**	–	Hemizygous	Intron 6	–	–	–	–	–	MaxEnt: −75.0% NNSPLICE: -25.1% HSF: −13.6%	FERM 3	**This study**

F, family; M, male; F, female.
Novel mutations are highlighted in bold.
* Proband.

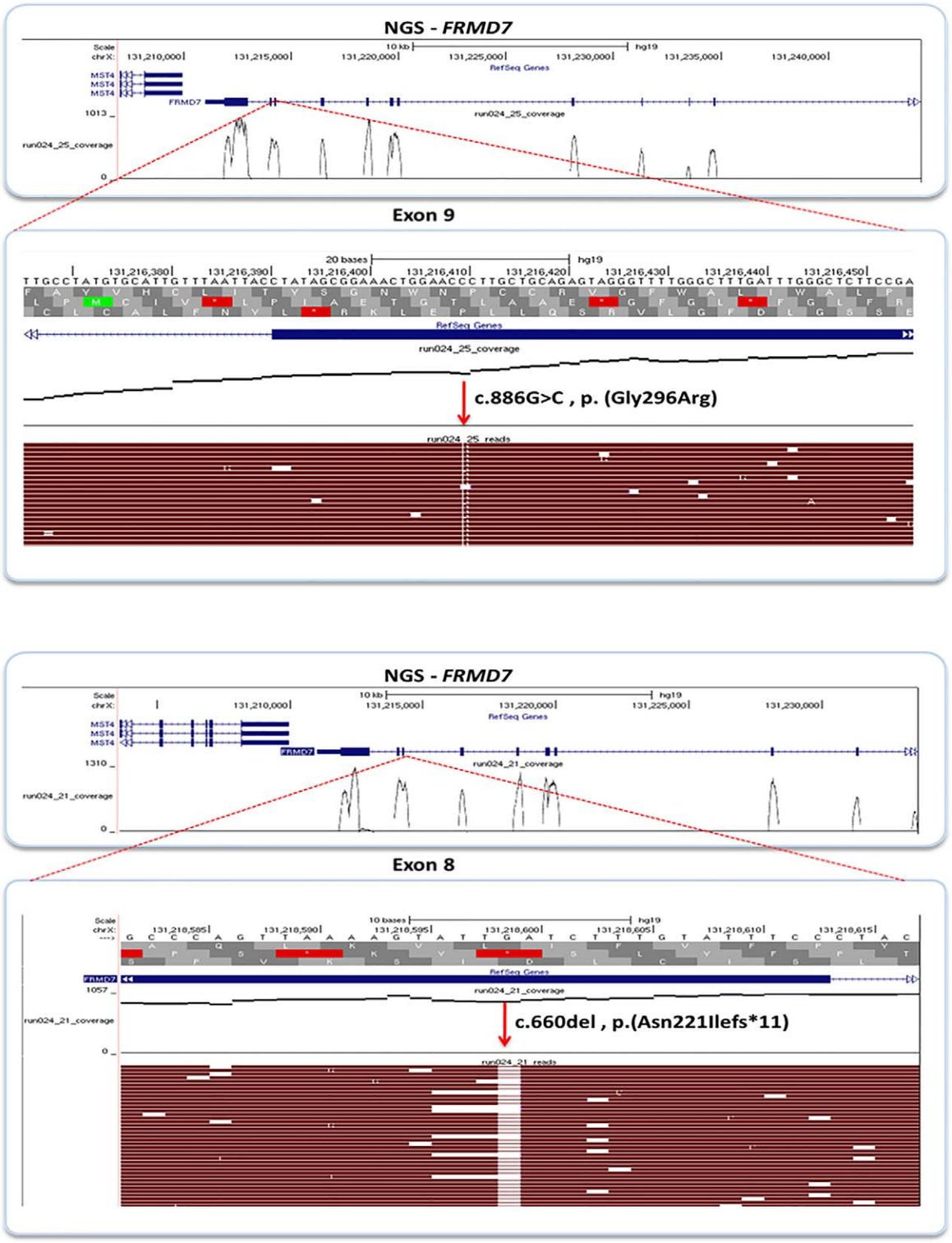

Figure 3. Illustration of targeted next generation sequencing (NGS) of the coding region of *FRMD7*. *Upper panel*: UCSC figure of the *FRMD7* genomic region with coding exons as *black rectangles*. The coverage of the different coding exons and intron boundaries are indicated below the exons. A detailed view is given of the region around mutation c.886G>C in exon 9 in individual II:1 (F3), with coverage of 25×. *Lower panel*: Similar representation of the mutation as described in the *upper panel*. The mutation c.660del in individuals IV:1*, V:7*, and V:1* (of F4, F5, and F6, respectively) is presented with a coverage of 21×.

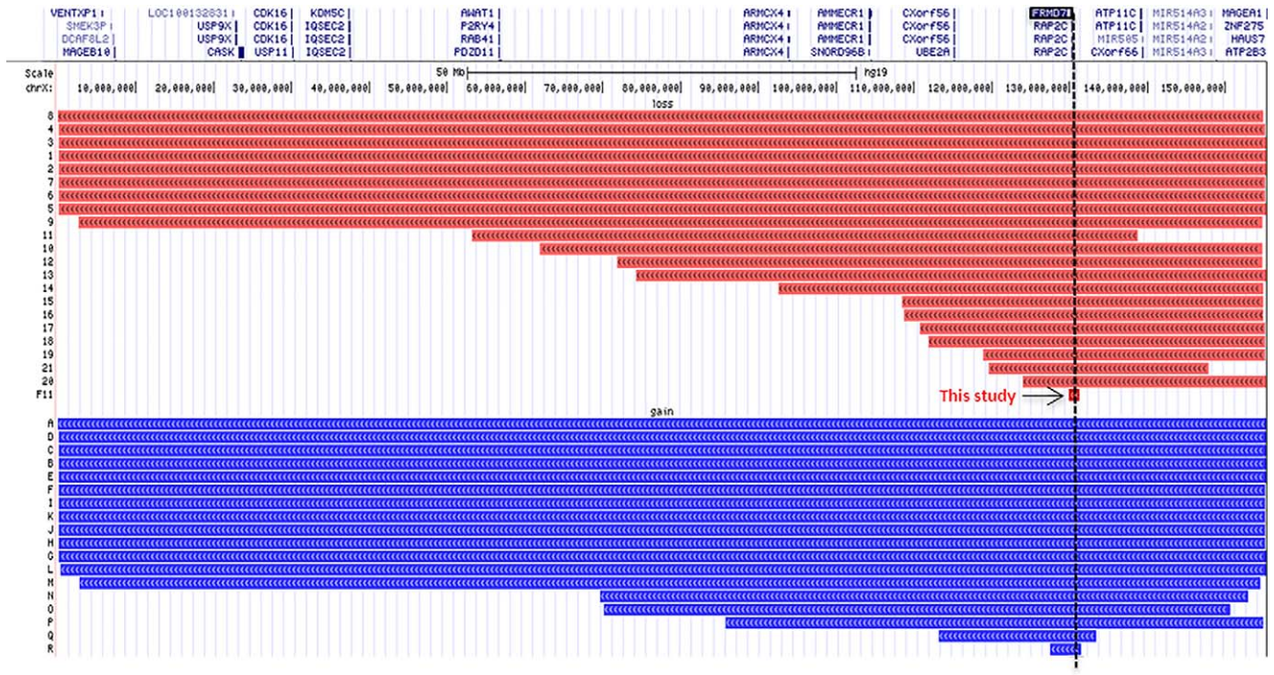

Figure 4. Overview of publicly available copy number variations of the *FRMD7* region and *FRMD7* encompassing deletion in F11. Overview of the X chromosome region (chrX:1–155,270,560; UCSC, Human Genome Browser, hg19) with custom tracks showing the CNVs and *FRMD7* encompassing deletion found in F11. At the *top*, the RefSeq Genes track is included. *Horizontal red bars* indicate deletions while *horizontal blue bars* indicate duplications. The location of *FRMD7* is indicated by a *vertical black line*. Additional information on the CNVs including the database, size, and the clinical phenotype can be found in Supplementary Table S2.

To date, seven unique mutations have been reported in exon 12 of *FRMD7*,[16] all of which are truncating. In this study, a novel frameshift mutation was found in this exon: c.2036del. Overall, this highlights an important role of the highly conserved C-terminal region of FRMD7.

Up to now, only one partial *FRMD7* deletion was described in FIN, spanning exons 2 to 4.[30] Here, we identified a deletion of 1.29 Mb in a male patient with nystagmus and autism, encompassing *FRMD7* and six other genes, only two of which have been associated with disease so far (i.e., *FRMD7* and *IGSF1*, respectively). It is unclear if the autism spectrum disorder can be explained by this X-chromosomal deletion. A search for other disease-associated CNVs of the *FRMD7* region in Decipher and our local CNV database revealed 22 losses and 18 gains of variable sizes, all larger than the deletion found here, and in patients with different phenotypes without mentioning of IIN. Hence, the deletion found here can be considered to be the first total *FRMD7* deletion reported in FIN (Fig. 4).

In the remainder of the patients with no identified *FRMD7* mutations or CNVs, we cannot exclude mutations in noncoding regions of *FRMD7* such as promoter or regulatory regions, deep intronic mutations, or mutations in other genes at different loci. In this respect, further cDNA studies on patients' lymphocytes[7] might be helpful to uncover noncoding mutations of *FRMD7*. Finally, whole-exome sequencing (WES) will be the next strategy to identify potential novel IIN genes in our unique discovery cohort of unexplained IIN cases.

The novelty of this study lies within the fact that we provide the third larger study, after the initial cloning paper of *FRMD7* by Tarpey et al.[7] and Thomas et al.,[6] which included familial as well as sporadic cases, investigating the role of *FRMD7* mutations in relation to IIN. Our study did not only reveal a number of novel mutations, but reports also, for the first time, a total gene deletion of *FRMD7* in FIN.

In conclusion, genetic defects of *FRMD7* including a genomic rearrangement were found in 11/49 (22.4%) probands, five of which are novel. Our study generates a discovery cohort of IIN patients harboring either undetected noncoding mutations of *FRMD7* or mutations in genes at known or novel loci sustaining the genetic heterogeneity of IIN.

Acknowledgments

The authors thank the families who participated in this study.

Supported by grants from the Saudi Arabia's King Abdullah Scholarship Program (Riyadh, Saudi Arabia; BAM), the Research Foundation Flanders (FWO; MB, HV, FCP, EDB, and BPL; Brussels, Belgium).

Disclosure: **B. AlMoallem**, None; **M. Bauwens**, None; **S. Walraedt**, None; **P. Delbeke**, None; **J. De Zaeytijd**, None; **P. Kestelyn**, None; **F. Meire**, None; **S. Janssens**, None; **C. van Cauwenbergh**, None; **H. Verdin**, None; **S. Hooghe**, None; **P. Kumar Thakur**, None; **F. Coppieters**, None; **K. De Leeneer**, None; **K. Devriendt**, None; **B.P. Leroy**, None; **E. De Baere**, None

References

1. Sarvananthan N, Surendran M, Roberts EO, et al. The prevalence of nystagmus: the Leicestershire nystagmus survey. *Invest Ophthalmol Vis Sci*. 2009;50:5201–5206.
2. Papageorgiou E, McLean RJ, Gottlob I. Nystagmus in childhood. *Pediatr Neonatol*. 2014;55:341–351.
3. Hackett A, Tarpey PS, Licata A, et al. CASK mutations are frequent in males and cause X-linked nystagmus and variable XLMR phenotypes. *Eur J Hum Genet*. 2010;18:544–552.

4. Zhou P, Wang Z, Zhang J, Hu L, Kong X. Identification of a novel GPR143 deletion in a Chinese family with X-linked congenital nystagmus. *Mol Vis*. 2008;14:1015–1019.
5. Liu JY, Ren X, Yang X, et al. Identification of a novel GPR143 mutation in a large Chinese family with congenital nystagmus as the most prominent and consistent manifestation. *J Hum Genet*. 2007;52:565–570.
6. Thomas S, Proudlock FA, Sarvananthan N, et al. Phenotypical characteristics of idiopathic infantile nystagmus with and without mutations in FRMD7. *Brain*. 2008;131;1259–1267.
7. Tarpey P, Thomas S, Sarvananthan N, et al. Mutations in FRMD7, a newly identified member of the FERM family, cause X-linked idiopathic congenital nystagmus. *Nat Genet*. 2006;38: 1242–1244.
8. Thomas MG, Crosier M, Lindsay S, et al. Abnormal retinal development associated with FRMD7 mutations. *Hum Mol Genet*. 2014;23:4086–4093.
9. Zhang Q, Xiao X, Li S, Guo X. FRMD7 mutations in Chinese families with X-linked congenital motor nystagmus. *Mol Vis*. 2007;13:1375–1378.
10. Thomas NS, Harris CM, Hodgkins PR. Allelic variation of the ophthalmic molecular genetics. *Ophthalmic Mol Genet*. 2007; 125:1255–1263.
11. Migeon BR. Why females are mosaics, X-chromosome inactivation, and sex differences in disease. *Gender Med*. 2007;4: 97–105.
12. Chishti AH, Kim AC, Marfatia SM, et al. The FERM domain: a unique module involved in the linkage of cytoplasmic proteins to the membrane. *Trends Biochem Sci*. 1998;23:281–282.
13. Baines AJ. A FERM-adjacent (FA) region defines a subset of the 4.1 superfamily and is a potential regulator of FERM domain function. *BMC Genomics*. 2006;20:85.
14. Pu J, Lu X, Zhao G, et al. FERM domain containing protein 7 (FRMD7) upregulates the expression of neuronal cytoskeletal proteins and promotes neurite outgrowth in Neuro-2a cells. *Mol Vis*. 2012;18:1428–1435.
15. Watkins RJ, Patil R, Goult BT, Thomas MG, Gottlob I, Shackleton S. A novel interaction between FRMD7 and CASK: evidence for a causal role in idiopathic infantile nystagmus. *Hum Mol Genet*. 2013;22:2105–2118.
16. Schouten JP, McElgunn CJ, Waaijer R, Zwijnenburg D, Diepvens F, Pals G. Relative quantification of 40 nucleic acid sequences by multiplex ligation- dependent probe amplification. *Nucleic Acids Res*. 2002;30:e57.
17. Kelley LA, Sternberg MJ. Protein structure prediction on the Web: casestudy using the Phyre server. *Nat Protoc*. 2009;4: 363–371.
18. Cho W, Stahelin RV. Membrane-protein interactions in cell signaling and membrane trafficking. *Annu Rev Biophys Biomol Struct*. 2005;34:119–151.
19. De Leeneer K, Hellemans J, Steyaert W, et al. Flexible, scalable and efficient targeted resequencing on a benchtop sequencer for variant detection in clinical practice [published online ahead of print December 12, 2014]. *Hum Mutat*. doi:10.1002/humu.22739.
20. Oostlander AE, Meijer GA, Ylstra B. Microarray-based comparative genomic hybridization and its applications in human genetics. *Clin Genet*. 2004;66:488–495.
21. Liu Z, Mao S, Pu J, Ding Y, Zhang B, Ding M. A novel missense mutation in the FERM domain containing 7 (FRMD7) gene causing X-linked idiopathic congenital nystagmus in a Chinese family. *Mol Vis*. 2013;19:1834–1840.
22. Li N, Wang L, Cui L, et al. Five novel mutations of the FRMD7 gene in Chinese families with X-linked infantile nystagmus. *Mol Vis*. 2008;14:733–738.
23. Zhang X, Ge X, Yu Y, et al. Identification of three novel mutations in the FRMD7 gene for X-linked idiopathic congenital nystagmus. *Sci Rep*. 2014;4:3745.
24. Thusberg J, Vihinen M. Pathogenic or not? And if so, then how? Studying the effects of missense mutations using bioinformatics methods. *Hum Mutat*. 2009;30:703–714.
25. Barnes MR. *Bioinformatics for Geneticists: A Bioinformatics Primer for the Analysis of Genetic Data*. 2nd ed. Hoboken, NJ: Wiley; 2007.
26. Burley SK, Petsko GA. Aromatic-aromatic interaction: a mechanism of protein structure stabilization. *Science*. 1985; 229:23–28.
27. Lanzarotti E, Biekofsky RR, Estrin DA, Marti MA, Turjanski AG. Aromatic-aromatic interactions in proteins: beyond the dimer. *J Chem Inf Model*. 2011;51:1623–1633.
28. Reid, KSC, Lindley, PF, Thornton, JM. Sulfur-aromatic interactions in proteins. *FEBS Lett*. 1985;190:209–213.
29. Wagner SA, Beli P, Weinert BT, et al. Proteomic analyses reveal divergent ubiquitylation site patterns in murine tissues. *Mol Cell Proteomics*. 2012;11:1578–158
30. Fingert JH, Roos B, Eyestone ME, Pham JD, Mellot ML, Stone E. Novel intragenic FRMD7 deletion in a pedigree with congenital X-linked nystagmus. *Ophthalmic Genet*. 2010;31:77.

ED: Please verify the accuracy of any edits made to the article summary below.

We expanded the molecular pathogenesis of *FRMD7*-related idiopathic infantile nystagmus (FIN) using a comprehensive molecular approach. Apart from novel coding mutations this revealed a genomic rearrangement of the *FRMD7* locus in FIN.

Investigative Ophthalmology & Visual Science